SERBIAN JOURNAL OF ELECTRICAL ENGINEERING
Vol. 8, No. 1, February 2011, 53-62

UDK: 537.874

Electronic States and Optical Transitions in a Graphene Quantum Dot in a Normal Magnetic Field*

Marko Grujić[1], Milan Tadić[1]

Abstract: An analytical approach using the Dirac-Weyl equation is implemented to obtain the energy spectrum and optical absorption of a circular graphene quantum dot in the presence of an external magnetic field. The results are obtained for the *infinite-mass* and *zigzag* boundary conditions. We found that the energy spectra of a dot with zigzag boundary condition exhibit a zero energy band regardless of the value of the magnetic field, while for the infinite mass boundary conditions, the zero energy states appear only for high magnetic fields.

Keywords: Graphene, Circular, Quantum dot.

1 Introduction

Graphene is an allotrope of carbon which, due to its novel properties, has attracted considerable attention recently [1, 2]. The energy spectrum of graphene is linear at two inequivalent points (K and K') in the Brillouin zone. Such a linear behavior is a characteristic of relativistic massless particles, which can be studied using the Dirac-Weyl equation [3]. The manipulation of charge carrier states in graphene can be made either by using external magnetic fields, which lead to the appearance of Landau levels for an infinite graphene sheet, or by using finite size graphene quantum dots (GQD's) [4].

Edge termination plays a major role in the energy spectrum of graphene. For a zigzag termination in graphene nanoribbons and graphene flakes, such as triangular and hexagonal GQD's, a band of zero-energy edge-localized states is found [5, 6]. Except for the case where all the terminations of the graphene flake are armchair, the appearance of the zero energy states seems to be robust with respect to the edge roughness, as demonstrated by the persistent finite density of these states observed in realistic quasi-circular GQD's [7].

It has been shown that graphene structures with zigzag segments on the edge are prone to spontaneous magnetic ordering, which can be approximately

[1]School of Electrical Engineering, University of Belgrade, P.O. Box 3554, 11120 Belgrade, Serbia;
E-mails: marko.grujic@etf.bg.ac.rs; milan.tadic@etf.bg.ac.rs

*Award for the best paper presented in Section *Microelectronics and Optoelectronics*, at Conference ETRAN 2010, June 7-11, Donji Milanovac, Serbia.

treated by imposing the infinite mass boundary condition (IMBC) [8-10]. Recent calculations, however, suggest that the edge magnetization is not a robust property of the GQD. Several different factors might lead to the suppression of edge magnetization, such as impurities and edge defects [11, 12], the thermal instability of the lattice and the spontaneous edge reconstruction [12-14]. In the latter, even though the edge magnetism is suppressed, the edge states near the Fermi energy remain. Hence, the applications of the zigzag boundary condition (ZZBC) to the circular GQD's seem to be more appropriate than the IMBC. However, if the spontaneous edge reconstruction could be suppressed by any means (like adsorbing the hydrogen atoms) [12], the application of the IMBC would be a better choice. Therefore, it is our goal to analyze and compare properties stemming from the two boundary conditions.

In this paper, we analytically solve the Dirac-Weyl equation for a circular graphene quantum dot under a perpendicular magnetic field, for both infinite-mass and zigzag boundary conditions. A comparison between the energy spectra for each boundary condition is made. Furthermore, we discuss the effect of a magnetic field on the optical spectrum of a circular GQD, where we analyze the effect of different boundary conditions (i.e. ZZBC and IMBC) on the interband optical transition.

2 The Continuum Approach

The Dirac-Weyl Hamiltonian for low-energy electron states in graphene, in the presence of a perpendicular magnetic field and a mass-related potential, reads

$$H = v_F(\boldsymbol{p} + e\boldsymbol{A})\boldsymbol{\sigma} + V(r)\sigma_z . \tag{1}$$

Here $\boldsymbol{\sigma}$ denotes the pseudo-spin Pauli matrix, which takes into account contributions of two different graphene sublattices. This equation holds for the K valley states, and one should employ $\boldsymbol{\sigma}^*$ to consider states in the K' valley. We assume that the carriers are confined in a circular area of radius R, so that $V(r) = 0$ for $r < R$, and $V(r) \to \infty$ for $r \geq R$, where r is the radial coordinate of the cylindrical coordinates system. In the case of the adopted ZZBC, the two Dirac cones are labeled by the quantum number k, which has the value $+1$ in the K valley, and -1 in the K' valley. For the IMBC, however, we use the so called valley-isotropic form of the Hamiltonian, with fixed $k = +1$, and the valleys are differentiated by another quantum number τ, which is employed in the boundary condition itself. Furthermore, we introduce the dimensionless variables $\rho = r / R$, $\beta = R^2 / 2l_B^2 = eBR^2 / 2\hbar$ and $\varepsilon = E / E_0 = ER / \hbar v_F$, where

E is the carrier energy, v_F is the Fermi velocity, and l_B is the magnetic length. Since $[H, J_z] = 0$, the total angular momentum is a conserved quantity, and thus the two-component wave function has the form:

$$\psi(r,\phi) = \mathrm{e}^{\mathrm{i}m\phi}\begin{pmatrix} \chi_1(r) \\ \mathrm{e}^{\mathrm{i}k\phi}\chi_2(r) \end{pmatrix}. \tag{2}$$

where $m = 0, \pm 1, \pm 2, \ldots$ is the angular momentum quantum number. The following boundary conditions

$$\frac{\psi_2(R,\phi)}{\psi_1(R,\phi)} = \mathrm{i}\tau\mathrm{e}^{\mathrm{i}\phi}, \tag{3}$$

$$\psi_1(R,\phi) = 0. \tag{4}$$

are examined. The form in (3) is called the infinite mass boundary condition (IMBC), where $\tau = +1(-1)$ is employed for the $K(K')$ states. The condition in (4) requires one of the wave function components to be equal to zero at the dot edge, and is called the zigzag boundary condition (ZZBC). The applicability of ZZBC is known to span a wide range of edge terminations, containing mixed zigzag and armchair boundaries, contrary to the armchair boundary condition, being applicable only to a small subset of purely armchair terminated structures [15]. Neither IMBC nor ZZBC admixes valleys, as their eigenstates belong to one or the other valley exclusively.

2.1 Zero energy solutions

When $\varepsilon = 0$, the differential equations (1) are decoupled and offer straightforward solutions of the form:

$$\chi_1(\rho) = C_1\rho^{mk}\,\mathrm{e}^{k\beta\rho^2/2} \quad \text{and} \quad \chi_2(\rho) = C_2\rho^{-(mk+1)}\,\mathrm{e}^{-k\beta\rho^2/2}.$$

These solutions can not simultaneously satisfy the IMBC in (3) and be normalisable. Thus, there are no zero energy states in the IMBC spectrum.

If the ZZBC given by (3) is employed, it is possible to find the normalisable zero energy solutions in both valleys. Those wave function components have the form $\chi_1(\rho) = 0$ and $\chi_2(\rho) = C\rho^{-(mk+1)}\,\mathrm{e}^{-k\beta\rho^2/2}$, with $mk = -1, -2, -3, \ldots$ Obviously, these states are completely pseudo-spin polarized. The form of the wave function indicates that all states, except for $mk = -1$ ones, are edge localized. Furthermore, the states with the larger $|m|$ are localized closer to the edge.

2.2 Non-zero energy solutions for $\beta = 0$

When $\varepsilon \neq 0$ and $\beta = 0$, (1) requires decoupling and offers solutions of the Bessel type $\chi_1(\rho) = C_1 J_m(\varepsilon\rho)$. From (1), the relation between the first and the second component of the wave function follows

$$\psi_2(\rho,\phi) = \frac{\mathrm{e}^{\mathrm{i}k\phi}}{\varepsilon}\left(-i\partial_\rho + \frac{k}{\rho}\partial_\phi + ik\beta\rho\right)\psi_1(\rho,\phi), \tag{5}$$

and

$$\chi_2(\rho) = ikC_1 J_{m+k}(\varepsilon\rho). \tag{6}$$

The boundary condition (3) leads to the equation $\tau J_m(\varepsilon) = J_{m+1}(\varepsilon)$, while the boundary condition (4) gives $J_m(\varepsilon) = 0$. Recalling that the Bessel functions obey properties $J_m(\varepsilon) = (-1)^m J_{-m}(\varepsilon)$ and $J_m(\varepsilon) = (-1)^m J_m(-\varepsilon)$, several interesting properties of the zero-field energy spectra are derived: i) for the ZZBC, the states of equal m in both valleys have the same energy, whereas for the IMBC, the m states in the K valley have equal energies to the $-(m+1)$ states in the K' valley; ii) for the ZZBC, positive and negative energy m states are symmetric with respect to $\varepsilon = 0$, whereas for the IMBC, similar symmetry between the positive energy m states and negative energy $-(m+1)$ states is found. This latter property indicates that the intervalley electron-hole symmetry between the states of the same m is present when the IMBC is adopted. iii) According to i) and ii) we may deduce that the energy spectrum within each valley is either doubly degenerate (for $m \neq 0$) or non-degenerate (for $m = 0$) if the ZZBC is adopted. This is not a case when the IMBC is adopted.

2.3 Non-zero energy solutions for $\beta \neq 0$

For the general case $\varepsilon \neq 0$ and $\beta \neq 0$, the normalisable solution is

$$\psi_1(\rho,\phi) = C\,\mathrm{e}^{\mathrm{i}m\phi}\,\rho^m\,\mathrm{e}^{-\beta\rho^2/2}\,{}_1\widetilde{F}_1\left(\frac{2m+k+1}{2} - \frac{\varepsilon^2}{4\beta}, m+1, \beta\rho^2\right), \tag{7}$$

where we used the relation $\psi_1(\rho,\phi) = \mathrm{e}^{\mathrm{i}m\phi}\chi_1(\rho)$, obtained from (1) and (2), and ${}_1\widetilde{F}_1(a,b,z)$ is the regularized confluent hypergeometric function. Having extracted the second component of the wave function from (5), the IMBC leads to the following eigenvalue equation:

$$\frac{\tau\varepsilon}{2}\,{}_1\widetilde{F}_1\left(m+1-\frac{\varepsilon^2}{4\beta}, m+2, \beta\right) - {}_1\widetilde{F}_1\left(m+1-\frac{\varepsilon^2}{4\beta}, m+1, \beta\right) = 0, \tag{8}$$

while for the ZZBC we obtain

$$ {}_1\widetilde{F}_1\left(\frac{2m+k+1}{2}-\frac{\varepsilon^2}{4\beta},m+1,\beta\right)=0. \tag{9}$$

One may notice that the positive-energy K and negative-energy K' spectra obtained from (8) are symmetric, since the choice $\varepsilon>0$ and $\tau=+1$ produces the same eigenvalue equation as the choice $\varepsilon<0$ and $\tau=-1$. On the other hand, when the ZZBC is adopted, (9) depends on the ε^2, and consequently the electron and hole states in each valley exhibit symmetry.

2.4 Energy spectrum

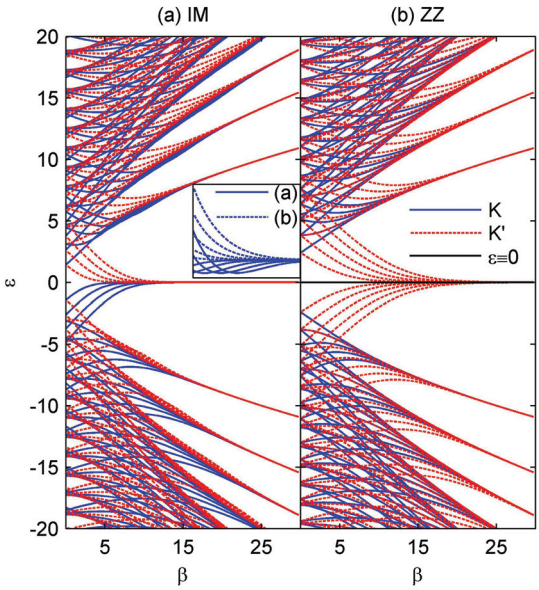

Fig. 1 – *Energy spectra of a circular graphene quantum dot in a perpendicular magnetic field for*: (a) *the* IMBC; (b) ZZBC.
The K valley spectrum is depicted by the solid blue lines, the K' spectrum is shown by the dashed red lines, while the zigzag zero energy band (ZES*) is shown by the solid black line. Inset shows how the quantum dot states merge to form the first LL in the K valleys for both adopted boundary conditions. Radius of the dot used in the calculation is $R = 70$ nm.*

The six lowest energy levels in the analyzed GQD for each m in the range $[-4,4]$ for the ZZBC and IMBC cases are shown in Figs. 1a and 1b, respectively, for a dot with radius $R = 70$ nm. The spectrum at the K valley is displayed by the solid blue lines, whereas the red-dashed lines denote the

energy levels at the K' valley spectrum. The zero energy localized zigzag state (ZES) is shown by the horizontal solid black line in Fig. 1b. As already pointed out, use of the IMBC is justified by the existence of the magnetization related confinement [16], which leads to the energy gap in the spectrum, as evident in Fig. 1a. The magnetic ordering at the dot edge breaks reversal symmetry, and thus the electron-hole symmetry for each valley is broken, even when an external magnetic field is absent. Therefore, the energies of the electron and hole states in a given valley are not mutually related. However, the magnetic ordering cannot break the intervalley electron-hole symmetry when the IMBC is adopted, and is demonstrated by the $\varepsilon_K = -\varepsilon_{K'}$ relationship in Fig. 1a [17].

Unlike the IMBC, the application of the ZZBC produces the ZES, composed of the $m \le -1$ states in the K valley, and $m \ge +1$ states in the K' valley (see Section 2.1). When the magnetic field increases, the quantum-dot states merge to form the Landau levels (LL's) of graphene. In contrast to semiconductors, the LL's in graphene are unevenly spaced and exhibit square-root dependence on the magnetic field [2]. For the IMBC, the first LL ($n = 1$) is composed out of $m \le 0$ states, and the higher energy ($n > 1$) LL's are formed out of $m < n$ states in both the K and K' valleys. Such a behavior is similar to semiconductor QD's [18]. This behavior is also true for the LL's in the K valley of the ZZBC, displayed as the solid lines in Fig. 1b. For the LL's in the K' valley of the ZZBC we observe that the condensation rule is $m \le n$. The $m \le 0$ states in the K' valley spectrum for the adopted ZZBC and the $m < 0$ states in both valleys for the applied IMBC form the zero energy ($n = 0$) Landau level (ZLL). We point out that for both IMBC and ZZBC, only one of the valleys contributes to the zeroth Landau level in each band, which is known to be the case in massive graphene, and is the reason behind the anomalous QHE [2]. However, if the IMBC is adopted there are no physical solutions at zero energy, therefore the quantum dot states which form the ZLL cannot have an exact zero energy in the employed continuum model with this boundary condition.

The asymptotic dependence of the energy levels for large β is given by

$$\varepsilon_{n_\rho, m}(\beta) = \pm\sqrt{4\beta n}. \tag{10}$$

Here the Landau level index is denoted by n. Furthermore, two different regimes of carrier confinement might be resolved: at low magnetic fields, the confinement is due to graphene termination (edge confinement). The influence of the edge is suppressed when the magnetic field is large, and the confinement becomes dominated by magnetic field. However, in the continuum model, no matter how high the magnetic field is, it will not suppress the zero energy band. ZES and it's degeneracy will persist throughout the magnetic confinement

regime in the ZZBC spectrum, while it's wave function is pushed inwards, toward the center of the dot (see Section 2.1). For both adopted boundary conditions, the transition between the two confinement regimes takes place as the magnetic field increases (see Fig. 1). We may define the transition points as the points where the energies of the states in the quantum dot differ negligibly from the LL energy. Such defined transitions shift towards a larger magnetic field when $|m|$ increases. The displayed dependence of the energy levels in the analyzed circular GQD is consistent with experiments [19], which have shown that the Landau levels in graphene indeed possess a square root dependence on the magnetic field, and also prove the existence of the $n = 0$ LL at the Dirac charge neutrality point. We should note that the observed dependence of the electron and hole energy levels on magnetic field differ from the one in semiconductor quantum dots, where neither ZES nor $n = 0$ LL are found, and the Landau levels increase linearly with β. Moreover, energies of the negative m states obtained from (9) have a tendency to undershoot the positive m energies of the same Landau level, which is not the case of solutions of (10), as the inset in Fig. 1a displays.

2.5 Optical absorption

Optical absorption, for transition between states i and j, is measured by

$$\left|M_{ij}\right|^2 = |\langle \Psi_i | re^{i\phi_p} | \Psi_j \rangle|^2 . \tag{11}$$

Having calculated the matrix elements describing the transition for each possible pair of states, we introduced the Lorentzian-type broadening for the absorption spectrum, and also Fermi-Dirac statistics. The spectrum broadening parameter is assumed to be 1 meV in our calculations. The total absorption spectrum is taken to be the sum of all individual transitions $A(E) = \sum_{i,j} A_{i,j}(E)$ for both valleys. The integral with respect to ϕ is finite when $m_j = m_i$. Furthermore, no selection rule applies to n, which contradicts the case of massive graphene, where the transitions are allowed only between adjacent Landau levels [20].

Although transitions between states which do not differ by ± 1 in the value of n are allowed in the GQD, we found that their contribution to the overall absorption is a few orders of magnitude smaller than the contribution of the $n \to n \pm 1$ transitions. The matrix elements between the six lowest energy states for m in the range $[-4,+4]$ are taken into account when computing the absorption spectra. The absorption spectra for $\varepsilon_F = 0$ and three values of the magnetic field, $\beta = 5$, 10, and 15, are shown in the left and right panel of Fig. 2

for $T = 100$ and $T = 300$ K, respectively. The strongest absorption line is due to the $n = -1 \to n = 0$ and $n = 0 \to n = 1$ transitions for the IMBC and for transitions between ZES and $n = \pm 1$ LL for the ZZBC.

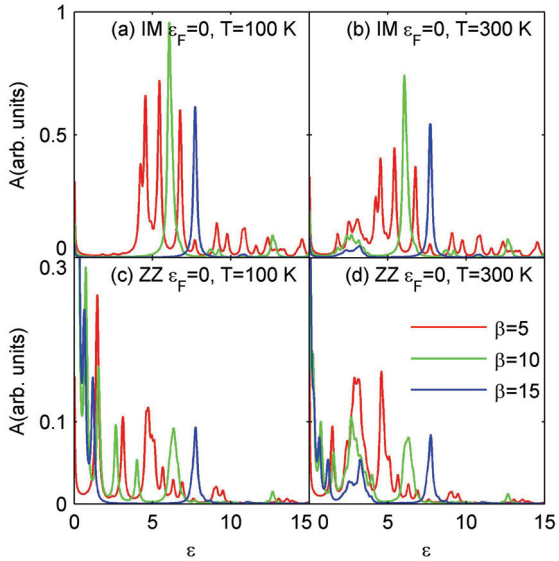

Fig. 2 – *The absorption spectrum* $A(\varepsilon)$ *for* $\varepsilon_F = 0$, *and both boundary conditions. Left and right panels correspond to temperatures* $T = 100$ K *and* 300 K: (a) $\varepsilon_F = 0$, $T = 100$ K; (b) $\varepsilon_F = 0$, $T = 300$ K; (c) $\varepsilon_F = 0$, $T = 100$ K; (d) $\varepsilon_F = 0$, $T = 300$ K.

The absorption spectra for the ZZBC Fig. 2c and 2d, display similar features as the absorption for the IMBC. In addition to the bright spot, the absorption spectra for both applied boundary conditions exhibit the bright and narrow absorption line, which is stronger for the IMBC. This absorption takes place by means of the $n = -1 \to n = 0$ and $n = 0 \to n = 1$ transitions in the case of the IMBC. For this case, the energies of the transitions between the states in the two valleys are equal, which is favorable for the appearance of this line. On the other hand, for the adopted ZZBC the energy spectrums of the electron and hole are symmetric within each valley, whereas the intervalley electron-hole symmetry does not exist. It leads to less pronounced central absorption peak in the spectrum, which is due to transitions between the ZES and $n = \pm 1$ LL in the both valleys. The other noteworthy feature for the ZZBC and $\varepsilon_F = 0$ is the absorption due to the interband transitions between the $n = 0$ quantum-dot states in the K' valley, whose transition energy tends to zero when the magnetic field increases.

3 Conclusion

The electron and hole states in a monolayer graphene circular quantum dot are modelled using the Dirac-Weyl equation. Two distinct types of boundary conditions are employed, namely the infinite-mass and the zigzag boundary conditions, which describe magnetic ordering at the edge and the edge reconstruction, respectively. The energy gap is found only for the infinite-mass boundary condition, whereas the peculiar zero energy state, which is pseudo-spin polarized and localized close to the zigzag boundary, exists when the zigzag boundary condition is adopted. Increase of the magnetic field diminishes influence of the edge on the electron confinement, and the states merge into Landau levels. The obtained spectra exhibit different symmetries between the electron and hole spectra, and also different intervalley symmetries.

Furthermore, the boundary conditions and the intervalley symmetry are found to influence the absorption spectra. Equal transition energies in the two valleys lead to the most intense absorption line for the adopted infinite mass boundary condition. On the other hand, different transitions energies in the two valleys lead to much smaller absorption if the zigzag boundary conditions are adopted.

4 Acknowledgment

This work was supported by the Ministry of Education and Science of Serbia.

5 References

[1] K.S. Novoselov, A.K. Geim, S.V. Morozov, D. Jiang, Y. Zhang, S.V. Dubonos, I.V. Grigorieva, A.A. Firsov: Electrical Field Effect in Atomically Thin Carbon Films, Science, Vol. 306, No. 5696, Oct. 2004, pp. 666 – 669.

[2] M.I. Katsnelson, K.S. Novoselov: Graphene: New Bridge between Condensed Mater Physics and Quantum Electrodynamics, Solid State Communication, Vol. 143, No. 1-2, July 2007, pp. 3 – 13.

[3] K.S. Novoselov, A.K. Geim, S.V. Morozov, D. Jiang, M.I. Katsnelson, I.V. Grigorieva, S.V. Dubonos, A.A. Firsov: Two-dimensional Gas of Massless Dirac Fermions in Graphene, Nature, Vol. 438, No. 7056, Nov. 2005, pp. 197 – 200.

[4] L.A. Ponomarenko, F. Schedin, M.I. Katsnelson, R. Yang, E.W. Hill, K.S. Novoselov, A.K. Geim: Chaotic Dirac Billiards in Graphene Quantum Dots, Science, Vol. 320, No. 5874, April 2008, pp. 356 – 358.

[5] K. Nakada, M. Fujita, G. Dresselhaus, M.S. Dresselhaus: Edge States in Graphene Ribbons: Nanometer Size Effect and Edge Shape Dependence, Physical Review B (Condensed Matter), Vol. 54, No. 54, Dec. 1996, pp. 17954 – 17961.

[6] H.P. Heiskanen, M. Manninen, J. Akola: Electronic Structure of Triangular, Hexagonal and Round Graphene Flakes near the Fermi Level, New Journal of Physics, Vol. 10, No. 10, Oct. 2008, 103015.

[7] M. Wimmer, A.R. Akhmerov, F. Guinea: Robustness of Edge States in Graphene Quantum Dots, Physical Review B, Vol. 82, No. 4, July 2010, 045409.

[8] H. Lee, Y.W. Son, N. Park, S. Han, J. Yu: Magnetic Ordering at the Edges of Graphitic Fragments: Magnetic Tail Interactions between the Edge-localized States, Physical Review B, Vol. 72, No. 17, Nov. 2005, 174431.

[9] J. Fernadez-Rossier, J. J. Palacios: Magnetism in Graphene Nanoislands, Physical Review Letters, Vol. 99, No. 17, Oct. 2007, 177204.

[10] D.P. DiVincenzo, E.J. Mele: Self-consistent Effective-mass Theory for Interlayer Screening in Graphite Intercalation Compounds, Physical Review B, Vol. 29, No. 4, Febr. 1984, pp. 1685 – 1694.

[11] B. Huang, F. Liu, J. Wu, B. Gu, W. Duan: Suppression of Spin Polarization in Graphene Naoribbons by Edge Defects and Impurities, Physical Review B, Vol. 77, No. 15, April 2008, 153411.

[12] J. Kunstmann, C. Ozdogan, A. Quandt, H. Fehske: Stability of Edge States and Edge Magnetism in Graphene Nanoribbons, Physical Review B, Vol. 83, No. 4, Jan. 2011, 045414.

[13] O. Voznyy, A.D. Guclu, P. Potasz, P. Hawrylak: Effect of Edge Reconstruction and Passivation on Zero-energy States and Magnetism in Triangular Graphene Quantum Dots with Zigzag Edges, Physical Review B, Vol. 83, No. 16, April 2011, 165417.

[14] P. Koskinen, S. Malola, K Hakkinen: Evidence for Graphene Edges beyond Zigzag and Armchair, Physical Review B, Vol. 80, No. 7, Aug. 2009, 073401.

[15] A.R. Akhmerov, C.W.J. Beenakker: Boundary Codition for Dirac Fermions on a Terminated Honeycomb Lattice, Physical Review B, Vol. 77, No. 8, Feb. 2008, 085423.

[16] C.L. Kane, E.J. Mele: Z2 Topological Order and the Quantum Spin Hall Effect, Physical Review Letters, Vol. 95, No. 14, Sept. 2005, 146802.

[17] S. Schnez, K. Ensslin, M. Sigrist, T. Ihn: Analytic Model of the Energy Spectrum of a Graphene Quantum Dot in a Perpendicular Magnetic Field, Physical Review B, Vol. 78, No. 19, Nov. 2008, 195427.

[18] C.S. Lent: Edge States in a Circular Quantum Dot, Physical Review B, Vol. 43, No. 5, Feb. 1991, pp. 4179 – 4186.

[19] D.L. Miller, K.D. Kubista, G.M. Rutter, M. Ruan, W.A. de Heer, P.N. First, J.A. Stroscio: Observing the Quantization of Zero Mass Carriers in Graphene, Science, Vol. 324, No. 5929, May 2009, pp. 924 – 927.

[20] V.P. Gusynin, S.G. Sharapov: Transport of Dirac Quadsiparticles in Graphene: Hall and Optical Conductivities, Physical Review B, Vol. 73, No. 24, 2006, 245411.